Mass- and Heat Transfer during Dissolution of Alumina

Asbjørn Solheim and Egil Skybakmoen

SINTEF, P.O. Box 4760 Torgarden, NO-7465 Trondheim, Norway

Key words: Alumina, Diffusion coefficient, Enthalpy, Mass transfer, Heat transfer

Abstract

Dissolution of alumina in industrial aluminium cells is a complicated process, not least because it involves formation of agglomerates, and it involves mass- and heat transfer phenomena taking place simultaneously. In the present study, the diffusion coefficient of alumina in cryolitic melts was measured using a rotating alumina disc. It was found that the temperature dependence of the diffusion coefficient is relatively large. The enthalpies for heating of alumina, conversion, and dissolution are summarised. The addition of 1 wt% alumina causes adiabatic cooling of typically 10-12 °C in a normal industrial bath. The dissolution can be regarded as being purely mass transfer controlled, since the heat required for dissolution only brings about 1 °C temperature drop from the bath bulk to the alumina surface. The bath at the alumina surface is saturated in alumina and has a lower liquidus temperature than the bulk. Alumina dissolution can, therefore, take place in a supercooled bath.

Introduction

Dissolution of alumina is a critical operation in the aluminium electrolysis. Modern technologies utilise point feeders, where alumina doses from a few hundred grams and up to two kilograms are added at regular intervals. Only a part of the dose dissolves immediately (the part dispersed as individual alumina grains). The rest of the dose may be carried through the bath in the form of lumps and agglomerates before it dissolves, it may rest on the metal surface, or it may fall to the bottom of the cell and form alumina sludge; see the illustration in Figure 1.

Since alumina is cold when it hits the bath surface, it will be encapsulated by frozen bath that must re-melt before the actual dissolution can start. At least a part of the alumina and frozen bath agglomerates to form a so-called "raft", which will float for a while before it eventually sinks [1]. Upon re-melting of the bath, the remaining alumina may form a dimensionally stable "skeleton" resulting from recrystallisation of γ-Al_2O_3 particles to form interlocking grains of α-Al_2O_3 [2]. The formation of rafts and lumps is the key factor in predicting the dissolution behaviour of industrial alumina. It turns out that alumina from different producers may behave quite differently in practice, but the behaviour can only to a limited degree be related to measured properties such as particle distribution, BET surface area, angle of repose, content of γ-Al_2O_3, etc.

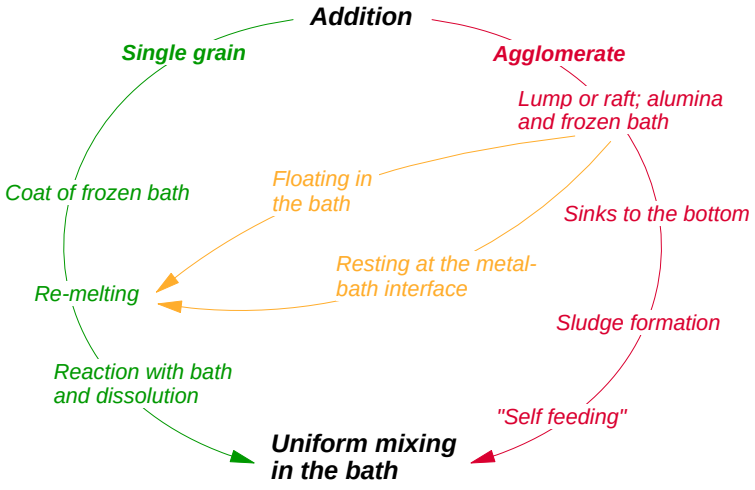

Figure 1. Paths for dissolution of alumina. The left-hand branch represents the rapid path.

Dissolution of alumina in a cryolitic melt is not a simple process. The solid alumina reacts with substances in the melt to form Al-O-F anions, and many such species have been suggested [3]. Still, when dealing with the bath in aluminium electrolysis cells, the melt structure is mainly of academic interest. The bath can be treated as a mixture of Na_3AlF_6, excess AlF_3, CaF_2 and Al_2O_3, and all necessary data are available in the form of empirical correlations. Since all properties including activity data are described in terms of concentrations or molar fractions of substances such as NaF, AlF_3, and Al_2O_3, it is not necessary to operate with two or more alumina species in an alumina dissolution model or in any other model.

The size and behaviour of agglomerates is probably the most important factor for the dissolution rate. Agglomeration is not well understood and difficult to predict quantitatively. Still, it is important to treat correctly the diffusion and heat transfer processes, which are the topics of the present paper. The enthalpies involved, the diffusion coefficient of alumina in cryolitic melts, and some features related to heat- and mass transfer phenomena in dissolution of alumina are summarised in the present paper.

Diffusion Coefficient for Alumina

Upon alumina feeding, a coat of frozen bath is formed around the alumina body, which has to re-melt to establish contact between alumina and the bath. It will be shown in a subsequent section that the time for freezing and re-melting is normally considerably shorter than the time for dissolution. The alumina reacts with the bath to form oxygen-containing anions, but the reaction is rapid. Therefore, the dissolution rate appears to be mass transfer controlled, which means that it depends on the diffusion coefficient for alumina.

In the present work as well as in the experiments by Gerlach et al. [4] and Frazer and Thonstad [5], rotating sintercorundum discs were used. Sintercorundum consists of pure α-Al_2O_3, while γ-Al_2O_3 is normally fed to the cell. The two structures will produce the same species of dissolved alumina, so there will be no difference in the rate of dissolution if it is mass transport controlled (mass transport control indicates that the chemical reactions involved are comparably fast). The rotating has a uniform mass transfer coefficient at the underside, and provided that the dissolution is mass transfer controlled, the rate of dissolution can be calculated by the equation derived by Levich [6]:

$$r_{diss} = 0.62\, D^{2/3} \nu^{-1/6} \omega^{1/2} \cdot \rho (w^* - w^\infty) \quad [kgm^{-2}s^{-1}] \qquad (1)$$

where D is the diffusion coefficient of alumina, ν is the kinematic viscosity of the bath, ω is the angular velocity of the disc, ρ is the bath density, and w is the mass fraction of alumina where "*" represents the surface (saturation) and "∞" represents the bulk (average during the experiment).

Experimental

A series of experiments with rotating sintered corundum discs were performed. The discs (30 mm dia. x 5 mm) were fastened to a steel rod and rotated at the surface of bath kept in a graphite crucible at rates varying from 56 to 260 rpm (angular velocity ω = 5.9-27.2 s^{-1}). Only the underside of the disc was in contact with the bath. The upper rotational rate was chosen so the conditions should be well below the limit for transition from laminar to turbulent flow (ω = 27 s^{-1} represents 10 percent of the critical Reynolds number). The time of rotation was varied in order to have approximately the same amount dissolved in each experiment. The temperature was measured by a type S thermocouple placed in the bath, protected by a stainless steel tube. After the experiment, the discs were cleaned mechanically and by means of a hot solution of aluminium chloride to remove adhering bath, and the rate of dissolution was determined from the weight loss.

The bath consisted of natural Greenland cryolite and aluminium fluoride sublimed in our own laboratory. The bath compositions, temperatures, density [7], viscosity [8], and alumina saturation [9] are given in Table 1.

Table 1. Bath compositions and temperatures used in experiments with rotating sintercorundum discs. The density [7] and the kinematic viscosity [8] were evaluated at the average of the alumina concentration at saturation [9] and the mean bulk concentration.

Experiment no.	1	2	3	4
Excess AlF_3 [wt%]	0	17.4	23.0	25.5
Temperature [°C]	1018 ± 2	959 ± 1	900 ± 1	852 ± 2
Al_2O_3(sat) [wt%]	12.96	8.37	5.98	4.68
Density [kgm^{-3}]	2042	1981	1976	1990
Kinematic viscosity x 10^6 [m^2s^{-1}]	1.22	1.01	0.95	0.98

Results

According to Levich (Equation 1), a plot of dissolution rate *vs*. the square root of the angular velocity would produce straight lines through the origin when the process is diffusion controlled. This was indeed the case for all temperatures, also the lowest temperature, as shown in Figure 2. The diffusion coefficient can be calculated from the slopes (B) of the lines in Figure 2 and data from Table 1,

$$B = 0.62\, D^{2/3} \nu^{-1/6} \omega^{1/2} \cdot \rho \qquad (2)$$

The diffusion coefficient usually varies exponentially with the temperature,

$$D = D_0 \cdot \exp\left(\frac{-E_D}{RT}\right) \qquad (3)$$

where D_0 is a constant, E_D is the activation energy for diffusion, R is the universal gas constant, and T is absolute temperature.

Figure 3 shows an Arrhenius-type plot of the calculated diffusion coefficients. The trend line, which was based on all the data shown in the figure, corresponds to an activation energy E_D = 79 485 J mol^{-1} and the constant D_0, based on a best fit of all the data, is $2.45 \cdot 10^{-6}$ m^2s^{-1} (see Equation 3). The activation energy appears to be relatively large when compared with other molten salt systems [11], which contributes to sluggish alumina dissolution in low-melting baths.

As can be observed in Figure 3, there is remarkably good agreement between the different sets of data. When calculating the diffusion coefficient for all individual measurements in the present work and using the activation energy E_D given above, the calculated constant D_0 was $(2.50 \pm 0.26) \cdot 10^{-6}$ m^2s^{-1}. This indicates an uncertainly (standard deviation) of about 11 percent. However, it should be mentioned that the present work does not fulfil the strict experimental requirements in using a rotating disc; e.g., the disc should be encapsulated by an inert material with considerably larger diameter than the disc. This might have entailed a systematic error not included in the 11 percent uncertainly mentioned above. It is difficult to know how large the error is. Still, the good agreement with the chronopotentiometric measurements by Thonstad [10] may indicate that the experimental shortcomings are not critical.

According to the results by Gerlach et al. [4], the diffusion coefficient does not vary much with the bath composition, and the present results were obtained with a large range of excess AlF_3. At normal cell conditions and temperature (950-970 °C) the value $D \approx 1.0 \cdot 10^{-9}$ m^2s^{-1} can be recommended.

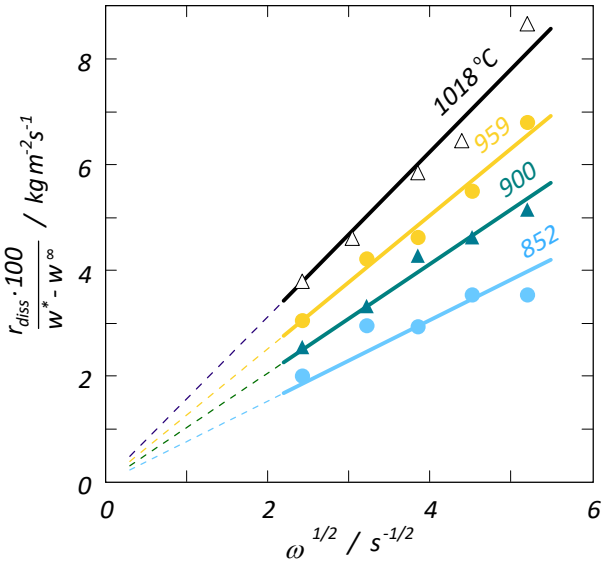

Figure 2. Rate of dissolution of sintered corundum discs as a function of the square root of the angular velocity at different temperatures and excess amounts of AlF_3 (see the text and Table 1).

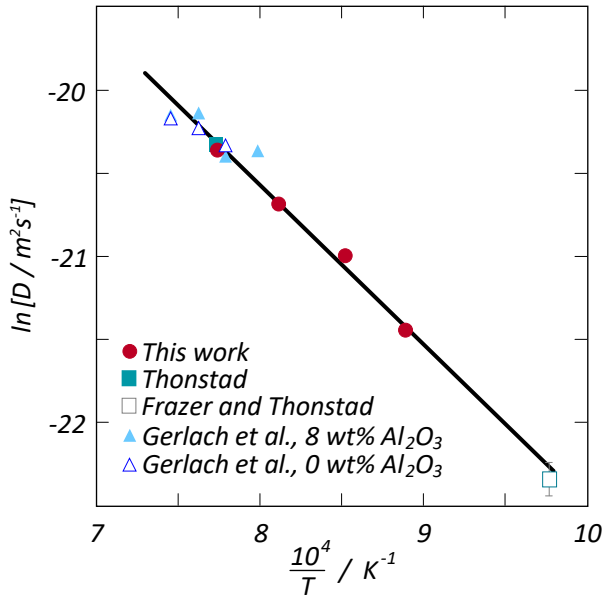

Figure 3. Arrhenius-type plot of the diffusion coefficient of alumina in cryolitic melts as a function of temperature. Data obtained by rotating sintercorundum discs, except Thonstad [10] (chronopotentiometry).

Enthalpies in Alumina Dissolution

Alumina produced by the Bayer process contains mainly γ-Al_2O_3 (normally above 95 percent), while α-Al_2O_3 is the thermodynamically stable crystalline form. The two alumina structures have somewhat different heat capacities. The γ-α transformation is exothermic. In vacuum or inert gas, the γ-α phase transformation is very slow at low or moderate temperatures, but it is catalysed by fluorides [12]. Still, it is not certain that all γ-Al_2O_3 alumina is transformed to α-Al_2O_3 before dissolution. However; since enthalpy is a state function, the total heat in the process from γ-alumina at 298 K to dissolved alumina at cell temperature is independent of the path. In the present paper, it will be assumed that γ-Al_2O_3 is heated from room temperature to cell temperature, while the γ-α conversion takes place at cell temperature, ending up with 100 percent α-Al_2O_3 before dissolution. The heat of mixing is based on experiments with α-Al_2O_3.

Heating of γ-Al_2O_3

The following equations for calculating the specific heat capacity and the heat content of γ-Al_2O_3 were based on data from NIST-JANAF [13]:

$$C_p = 1.483 - \frac{199.3}{T} \qquad [\text{kJ kg}^{-1}\text{K}^{-1}] \tag{4}$$

$$H_T^0 - H_{298}^0 = 1.483 \cdot (T - 298) - 199.3 \cdot \ln\left(\frac{T}{298}\right) \quad [\text{kJ kg}^{-1}] \tag{5}$$

Heating from 298 K (25 °C) to 1233 K (960 °C) requires 1103.6 kJ/kg.

γ-α Conversion

The heat involved in the γ-α transformation was also taken from NIST-JANAF [13]. The data could be represented by the following equation:

$$\Delta H_{\gamma\alpha}^0 = -185.0 - 0.067 \cdot (T - 298) + 9.6 \cdot \ln\left(\frac{T}{298}\right) \quad [\text{kJ kg}^{-1}] \tag{6}$$

At 1233 K (960 °C) the enthalpy change is -234.0 kJ/kg (exothermal).

Dissolution

The heat of mixing of α-Al_2O_3(s) in molten cryolitic melts was measured by Holm [14] and others, see reference [15]. In the derivation of activity data [15], the heat of mixing was expressed by:

$$\Delta H^{mix} = 87.0 \cdot x + 0.7875(r-1)^2 \cdot \left\{1 - e^{-60x}\right\} \quad \text{kJ mol}^{-1} \tag{7}$$

where x is the molar fraction of alumina in the system NaF-AlF_3-Al_2O_3 and r is the NaF/AlF_3 molar ratio. Note that Equation 7 gives the heat of mixing per mole of mixture, not per mole alumina added. A graphical representation of Equation 7, recalculated to weight percent and heat per kg of bath-alumina mixture, is shown in Figure 4.

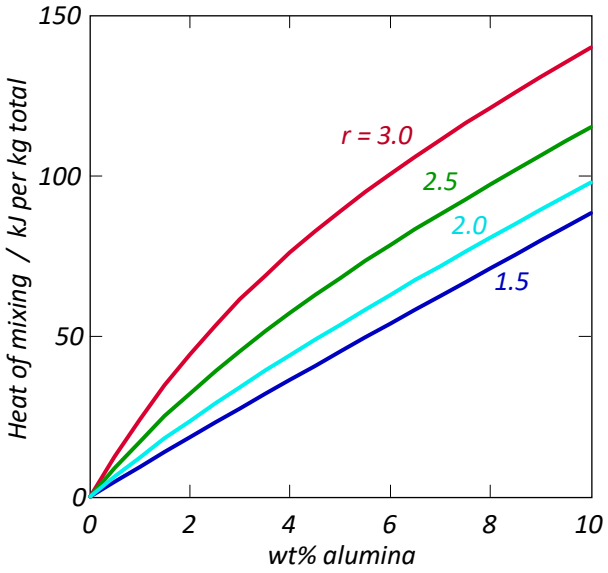

Figure 4. Heat of mixing as a function of the alumina concentration at different NaF/AlF_3 molar ratios.

Adiabatic Temperature Drop Upon Alumina Feeding

The heat requirements mentioned above lead to cooling of the bath when alumina is added. The heat capacity of cryolite is 1883 $Jkg^{-1}K^{-1}$ according to NIST-JANAF [13]. The data on other NaF-AlF_3 mixtures and melts containing CaF_2 and/or Al_2O_3 is very scarce, so the value for cryolite will be used in the following.

Figure 5 shows the calculated adiabatic temperature drop upon adding 1 kg alumina to 100 kg electrolyte, while Figure 6 illustrates the calculated liquidus temperature and the actual temperature when alumina is added to an industrial alumina-free melt. As can be observed; the effect on the actual bath temperature is stronger than the effect on the liquidus temperature. This means that alumina addition lowers the superheat, and eventually, bath will start freezing. This does not mean that the alumina dissolution stops, which will be discussed in a subsequent section.

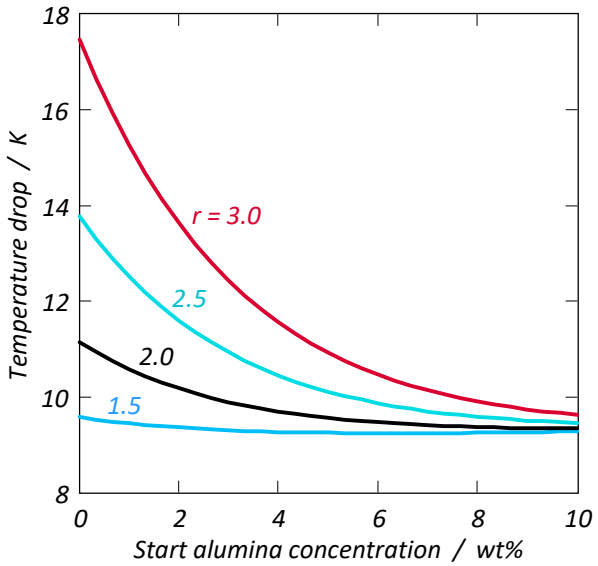

Figure 5. Temperature drop by addition of 1 kg alumina to 100 kg bath at different NaF/AlF_3 molar ratios, starting with γ-alumina. Heating of alumina from 298 K to 1233 K and γ-α conversion accounts for 4.6 K temperature drop.

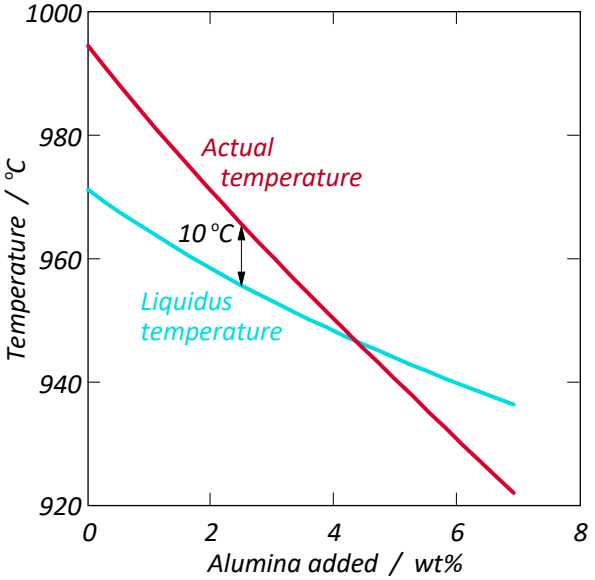

Figure 6. Liquidus temperature and actual temperature upon addition of alumina to industrial bath at adiabatic conditions. The superheat is 10 °C at 2.5 wt% Al_2O_3 and zero at 4.4 wt% Al_2O_3. The bath contains 12 wt% excess AlF_3 and 5.5 wt% CaF_2 at the origin.

Time for Re-Melting and Time for Dissolution

Ratio between Heat- and Mass Transfer Coefficients

Heat transfer and mass transfer are analogous phenomena, which entails that they can be treated by using the same dimensionless equations. Generally, forced convection heat transfer can be the expressed as a function of the dimensionless Nusselt number (Nu), Reynolds number (Re) and Prandtl number (Pr, see Table 2 for nomenclature and data):

$$Nu = C \cdot Re^{m} \cdot Pr^{1/3} \tag{8}$$

where C and m are constants depending of geometry and flow conditions. Mass transfer can be treated by the analogous equation

$$Sh = C \cdot Re^{m} \cdot Sc^{1/3} \tag{9}$$

Since the factors C, m, and characteristic dimension are equal in the two equations when applied to the same surface, the equations can be combined to give:

$$\frac{k}{h} = \frac{D}{\lambda} \cdot \left(\frac{Sc}{Pr} \right)^{1/3} \tag{10}$$

Using the data in Table 2 we obtain $k/h = 7.46 \cdot 10^{-9}$ $Km^3W^{-1}s^{-1}$.

For the dissolution of spheres, Nu = Sh = 2 at very low Reynolds numbers ($Re < 10^{-3}$), which gives $k/h = D/\lambda$.

Table 2. Nomenclature and data for mass- and heat transfer. The physicochemical data were evaluated at 960 °C for a bath containing 11.4 wt% excess AlF_3, 5.0 wt% CaF_2, and 4.0 wt% Al_2O_3 [8, 9, 13, 16].

Variable	Symbol/dimension	Value
Specific heat capacity	C_p [$Jkg^{-1}K^{-1}$	1883
Diffusion coefficient	D [m^2s^{-1}]	$1 \cdot 10^{-9}$
Heat transfer coefficient	h [$Wm^{-2}K^{-1}$]	-
Mass transfer coefficient	k [$kgm^{-1}s^{-1}$]	-
Characteristic length	L [m]	-
Flow velocity	u [ms^{-1}]	-
Kinematic viscosity	ν [m^2s^{-1}]	$1.26 \cdot 10^{-6}$
Thermal conductivity	λ [$Wm^{-1}K^{-1}$]	0.783
Density	ρ [kgm^{-3}]	2088
Nusselt number hL/λ	Nu [1]	-
Reynolds number uL/ν	Re [1]	-
Prandtl number $\rho C_p \nu/\lambda$	Pr [1]	6.33
Sherwood number kL/D	Sh [1]	-
Schmidt number ν/D	Sc [1]	1260

Re-Melting and Dissolution

Freezing and re-melting of bath formed on a cold alumina particle is a complicated dynamic process. In the present context, the purpose is to estimate the time for re-melting of the freeze as compared with the time for dissolution. As a simplification, we assume that there is an instant equilibration between the enthalpy needed for heating the alumina body and the enthalpy released by freezing bath onto the body.

The ratio between the time for re-melting ($t_{re\text{-}melt}$) and the time for dissolution (t_{diss}) then becomes:

$$\frac{t_{re-melt}}{t_{diss}} = \frac{m_{freeze} \cdot \Delta H_f}{A_{freeze} \cdot h \cdot \Delta T} \cdot \frac{A_{alumina} \cdot k \cdot \rho \Delta w}{m_{alumina}} \quad (11)$$

where m is mass and A is surface area. According to NIST-JANAF [13], the heat of freezing of cryolite (ΔH_f) is 507 kJ/kg at 1233 K. Heating of γ-Al_2O_3 from 298 to 1233 K and γ-α conversion requires 870 kJ/kg alumina (Eqs. 2 and 3). This means that there will be 870/507 = 1.7 kg frozen bath per kg alumina.

Provided that the convection is constant during re-melting and dissolution and that the surface area does not change much (i.e., a plate-shaped dimensionally stable raft), Equation 10 can be combined with Equation 11 to yield:

$$\frac{t_{re-melt}}{t_{diss}} = \frac{m_{freeze} \cdot \Delta H_f}{m_{alumina}} \cdot \frac{D}{\lambda} \cdot \left(\frac{Sc}{Pr}\right)^{1/3} \cdot \frac{\rho \Delta w}{\Delta T} \approx 13.5 \frac{\Delta w}{\Delta T} \quad (12)$$

where Δw and ΔT are the differences in mass fraction alumina and actual temperature, respectively, between the bulk and the surface.

Equation 12 indicates that the time for re-melting normally will be much shorter than the time for dissolution. As an example; if $\Delta w = 0.05$ (actual alumina concentration 5 wt% below saturation) and the superheat is 8 °C, the time for re-melting will be 8.4 percent of the time for dissolution. However, Equation 12 presupposed that the freeze layer exists as a separate "coat" on the exterior of the alumina body. This is probably not the case, unless the alumina body is non-porous. When there is freeze in between the alumina particles in a raft, melting may result in pieces falling off the raft, which was observed in a see-through laboratory cell by Yang et al. [16].

It should also be mentioned that it is not straightforward to assess the surface temperature of the alumina/freeze body during re-melting. Since the freeze is formed rapidly its composition is close to the bath, and the surface temperature is probably not equal to the liquidus temperature – which requires equilibrium between the bath and cryolite.

Alumina Surface Temperature During Dissolution

Actual Temperature

The ratio between the mass transfer coefficient and the heat transfer coefficient was established above, see Equation 10. The basic equations for mass- and heat transfer can be written

$$r_{diss} = k\rho(w^* - w^\infty) \quad (13)$$

and

$$q = h(T^* - T^\infty) = -r_{diss} \cdot H^{mix} \cdot h(T^* - T^\infty) \quad (14)$$

where H^{mix} is the heat of mixing, calculated per kg alumina dissolved. By combination of Eqs. 10, 13, and 14, we obtain:

$$T^\infty - T^* = \frac{D}{\lambda} \cdot \left(\frac{Sc}{Pr}\right)^{1/3} \rho H^{mix}(w^* - w^\infty) \quad (15)$$

Figure 7 shows the temperature difference between the bulk of the bath and the alumina surface during dissolution as a function of the alumina concentration. The result for a small sphere (where $k/h = D/\lambda$) is also shown. The temperature difference is negligible, since the lower temperature does not much affect the solubility of alumina; 1 °C corresponds to less than 0.04 wt% Al_2O_3. Therefore, the dissolution can be regarded as being purely mass transfer controlled.

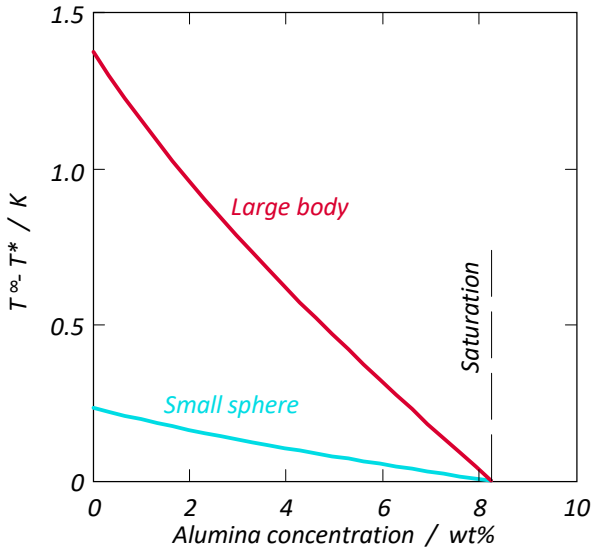

Figure 7. Temperature difference between the bulk and the alumina surface during dissolution as a function of the alumina concentration. NaF/AlF_3 molar ratio r = 2.2, 960 °C, 5.5 wt% CaF_2 at the origin.

Liquidus Temperature

The bath at the alumina surface will be saturated in alumina. The liquidus temperature "follows the concentration", which means that the liquidus temperature at the alumina surface may be much lower than the liquidus temperature in the bulk. Also, the diffusion boundary layer will be much thinner than the thermal boundary layer (the term $(Pr/Sc)^{1/3}$ is a rough measure of the relative thickness). Dissolution can take place even when the bulk of the melt is supercooled, as illustrated in Figure 8. Taking the bulk alumina concentration to be 3% Al_2O_3, the actual temperature is 0.8 °C lower at the surface than in the bulk (Figure 8), while the liquidus temperature is 21.7 °C lower [18].

The bulk of the bath may remain supercooled in the situation shown in Figure 8, but it is more likely that solid cryolite is formed on crystallisation sites in the bath, e.g., on the surface of carbon particles. This was suggested by Haupin [19] to explain the "superheat enigma", i.e., that the cell sometimes has apparently negative superheat.

Alumina will continue to dissolve at negative superheat, given that the bath temperature is above the border between primary crystallisation of cryolite and primary crystallisation of alumina (eutectic temperature in a binary mixture). Dissolution of alumina in a bath kept at its liquidus temperature was demonstrated by Thonstad et al. [20]. Figure 9 shows the eutectic temperature and alumina concentration as a function of the aluminium fluoride concentration.

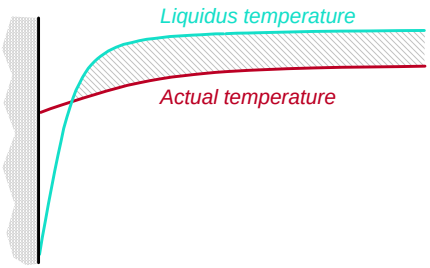

Figure 8. Schematic representation of the liquidus temperature and the bath temperature close to the surface of a dissolving alumina body. The shaded area is supercooled.

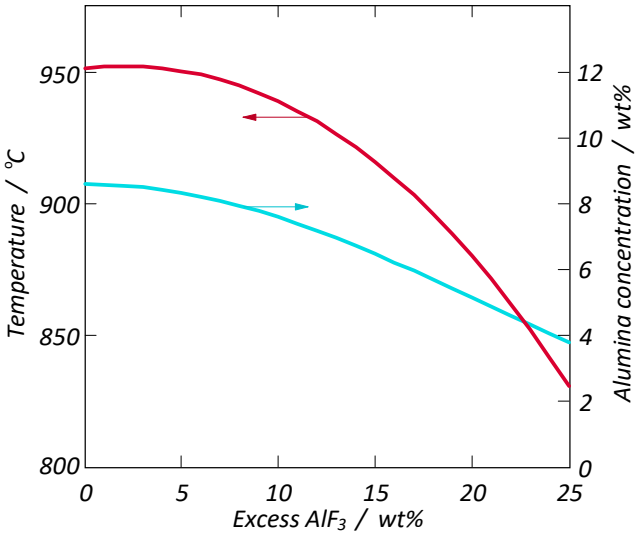

Figure 9. Temperature and alumina concentration at the border between primary crystallisation of cryolite and primary crystallisation of alumina as a function of the amount of excess aluminium fluoride. The bath contains 5.0 wt% calcium fluoride at all AlF_3 concentrations. Calculated from phase diagram data by Skybakmoen et al. [9] and by Solheim et al. [18].

Concluding Remark

The present work supports the common comprehension that dissolution of alumina in cryolitic melts is mass transport controlled, when the process has come so far that there is direct contact between alumina and bath. The total time for dissolution then depends on the size and nature of the agglomerates. Large agglomerates have a high volume to surface ratio, and larger dimensions also tend to give smaller mass- and heat coefficients. The tendency to break up in smaller pieces may, therefore, be important. Further work should focus on understanding the factors that govern agglomeration and the behaviour of agglomerates, which are related to the alumina itself as well as to the feeding parameters. The aim should be quantitative descriptions of the agglomerates. Predicting the time of dissolution for an alumina body with known size and density appears to be the easiest part in developing a CFD-based model for alumina dissolution.

Acknowledgement

The present work was mainly supported by SFI Metal Production, which is a Centre for Research-based Innovation financed by the Research Council of Norway and several end-users, among them Hydro Aluminium and Alcoa. Permission to publish the results is gratefully acknowledged.

References

1. S.E. Gylver, N.H. Omdahl, A.K. Prytz, A.J. Meyer, L.P. Lossius, and K.E. Einarsrud: Alumina Feeding and Raft Formation: Raft Collection and Process Parameters, Light Metals 2019, 659-666.
2. N.P. Østbø: Evolution of Alpha Phase Alumina in Agglomerates upon Addition to Cryolitic Melts, PhD Thesis, Norwegian University of Science and Technology (2002).
3. K. Grjotheim, C. Krohn, M. Malinovsky, *K. Matiasovsky, and J. Thonstad: Aluminium Electrolysis. Fundamentals of the Hall-Héroult Process*, 2nd Edition, Aluminium-Verlag, Düsseldorf, 1982, p.122.
4. J. Gerlach, U. Hennig und H.-D. Pöthsch: Zur Auflösungskinetik von Aluminiumoxid in Kryolithschmelzen mit Zusätzen von Al_2O_3, AlF_3, CaF_2, LiF oder MgF_2, *Erzmetall* **31** 496-504 (1978).
5. E.J. Frazer and J. Thonstad: Alumina Solubility and Diffusion Coefficient of the Dissolved Alumina Species in Low-Temperature Fluoride Electrolytes, *Met. Mater. Trans. B* **B41**(3) 543-548 (2010).
6. V.G. Levich: *Physicochemical Hydrodynamics (English translation)*. Prentice Hall, Englewood Cliffs, N. J., 1962.

7. A. Solheim: The Density of Molten NaF-LiF-AlF_3-CaF_2-Al_2O_3 in Aluminium Electrolysis, *Aluminum Transactions* **2** (1) 161-168 (2000).
8. T. Herzberg, K. Tørklep, and H.A. Øye: Viscosity of Molten NaF-AlF_3-Al_2O_3-CaF_2 Mixtures, *Light Metals 1980*, 159-170.
9. E. Skybakmoen, A. Solheim, and Å. Sterten: Alumina Solubility in Molten Salt Systems of Interest for Aluminium Electrolysis and Related Phase Diagram Data, *Met. Trans. B* **28B** 81-86 (1997).
10. J. Thonstad: Chronopotentiometry Measurements on Graphite Anodes in Cryolite-Alumina Melts, *Electrochim. Acta*, **14** 127-134 (1969).
11. G.J. Janz and N.P. Bansal: Diffusion Coefficients in Single and Multi-Component Salt Systems, *J. Phys. Chem. Ref. Data* **11**(3) (1982).
12. R. Ødegård, S. Rønning, S. Rolseth, and J. Thonstad: On Alumina Phase Transformation and Crust Formation in Aluminum Cells, *Light Metals 1984*, 695-709.
13. NIST-JANAF Thermochemical Tables, http://kinetics.nist.gov/janaf/
14. J.L. Holm: Thermodynamic Properties of Molten Cryolite and Other Fluoride Mixtures, Thesis, Institutt for uorganisk kjemi, NTH, Norway, 1971.
15. A. Solheim and Å. Sterten: Activity of Alumina in the System NaF-AlF_3-Al_2O_3 at NaF/AlF_3 Molar Ratios Ranging from 1.4 to 3, *Light Metals 1999*, 445-452.
16. V.A. Khoklov, E.A. Filatov, A. Solheim, and J. Thonstad: Thermal Conductivity in Cryolitic Melts - New Data and Its Influence on Heat Transfer in Aluminium Cells, *Light Metals 1998*, 501-506.
17. Y. Yang, B. Gao, Z. Wang, Z. Shi, and X. Hu: Study on the Dissolution of Alumina in Cryolite Electrolyte Using the See-Through Cell, *Light Metals 2015*, 583-588.
18. A. Solheim, S. Rolseth, E. Skybakmoen, L. Støen, Å. Sterten, and T. Støre: Liquidus Temperatures for Primary Crystallization of Cryolite in Molten Salt Systems of Interest for the Aluminium Electrolysis, *Met. Trans. B* **27B** 739-744 (1996).
19. W.E. Haupin: The Liquidus Enigma, *Light Metals 1992*, 477-480.
20. J. Thonstad, A. Solheim, S. Rolseth, and O. Skar: The Dissolution of Alumina in Cryolite Melts, *Light Metals 1988*, 655-661.